Chemical Science

EDGE ARTICLE

View Article Online
View Journal | View Issue

Cite this: *Chem. Sci.*, 2016, **7**, 2427

Selective capture of hexavalent chromium from an anion-exchange column of metal organic resin–alginic acid composite†

Sofia Rapti,‡[a] Anastasia Pournara,‡[a] Debajit Sarma,‡[b] Ioannis T. Papadas,[c] Gerasimos S. Armatas,[c] Athanassios C. Tsipis,[a] Theodore Lazarides,[d] Mercouri G. Kanatzidis[b] and Manolis J. Manos*[a]

Received 1st October 2015
Accepted 18th November 2015

DOI: 10.1039/c5sc03732h

www.rsc.org/chemicalscience

We report an anion exchange composite material based on a protonated amine-functionalized metal–organic framework, denoted Metal Organic Resin-1 (**MOR-1**), and alginic acid (**HA**). **MOR-1–HA** material shows an exceptional capability to rapidly and selectively sorb Cr(VI) under a variety of conditions and in the presence of several competitive ions. The selectivity of **MOR-1–HA** for Cr(VI) is shown to be the result of strong $O_3Cr^{VI}\cdots NH_2$ interactions. The composite sorbent can be successfully utilized in an ion-exchange column, in contrast to pristine **MOR-1** which forms fine suspensions in water passing through the column. Remarkably, an ion exchange column with only 1% wt **MOR-1–HA** and 99% wt sand (an inert and inexpensive material) is capable of reducing moderate and trace Cr(VI) concentrations to well below the acceptable safety limits for water. The relatively low cost of **MOR-1–HA**/sand column and its high regeneration capability and reusability make it particularly attractive for application in the remediation of Cr(VI)-bearing industrial waste.

Introduction

The contamination of water resources by toxic species represents a major cause of global concern. Among the most commonly found pollutants are various oxo-hydroxy anions.[1] A characteristic example is Cr(VI)-oxo species, found as dichromate ($Cr_2O_7^{2-}$), hydrogen chromate ($HCrO_4^-$) or chromate (CrO_4^{2-}) ions depending on the acidity/basicity of water. Cr(VI) is a well-known carcinogen, which is released to the environment from leather-tanning, cement, metal plating, dyes industries *etc.*[2] Commonly used and inexpensive methods such as precipitation of the ions from solution are not sufficiently effective to lower the concentration of Cr(VI) below the acceptable limits[3a,b] and they also generate large amounts of metal-containing sludge.[3c] Reduction of Cr(VI) to Cr(III) is a promising method, but presents some limitations such as generation of high concentrations of chromium(III) ions in the solution (a secondary treatment of the solution is then needed) or formation of solid waste (*e.g.* $Cr(OH)_3$).[4] Absorption and ion exchange are considered as highly effective and relatively inexpensive methods for the treatment of Cr(VI)-containing waste.[5] Several sorbents have been tested for this purpose. Organic resins, containing functional groups suitable for binding of specific cations or anions, are the most widely-used sorbents in various remediation processes and in the purification of drinking water.[5] Commercially available resins, with amine-functional groups, have shown promising Cr(VI) sorption properties.[6] Such materials, however, are not only of relatively high cost, but also absorb Cr(VI) through reduction–precipitation of Cr(III) species. Thus, such resins are actually oxidized–decomposed by Cr(VI) and they cannot be regenerated and reused. Furthermore, some tests indicated that these Cr(III)-loaded resins are not safe for disposal as non-hazardous solid waste due to significant Cr leaching.[6] On the other hand, layered double hydroxides (LDHs), the typical inorganic anionic exchangers, are inexpensive, but show relatively slow sorption kinetics for Cr(VI) and limited selectivity in the presence of competitive ions.[7]

Metal–organic frameworks (MOFs),[8] decorated with organic groups having strong binding affinity for toxic ions, may be ideal sorbents for various remediation processes. Such

[a]*Department of Chemistry, University of Ioannina, 45110 Ioannina, Greece. E-mail: emanos@cc.uoi.gr*

[b]*Department of Chemistry, Northwestern University, Evanston, IL 60208, USA*

[c]*Department of Materials Science and Technology, University of Crete, 71003 Heraklion, Greece*

[d]*Department of Chemistry, Aristotle University of Thessaloniki, 54124 Thessaloniki, Greece*

† Electronic supplementary information (ESI) available: Synthesis procedures, experimental details of physical measurements, SEM images, thermal analysis, CO_2 sorption data and pore size distribution, adsorption isotherms and details for the estimation of selectivity of **MOR-1–HA** for dichromate, IR spectrum, breakthrough curve in presence of excess of competitive ions and for **MOR-1–CA**, additional kinetic and characterization data, computational details and optimized geometries for $Ar\text{-}NH_3^+\cdots A$ complexes. See DOI: 10.1039/c5sc03732h

‡ These authors contributed equally.

functionalized materials, which can be prepared with facile methods and on a large scale, can be called metal–organic resins (**MORs**), since they combine the organic functionalities of the amorphous organic resins (strong binding groups)[5] and the ordered porous structure of crystalline MOFs. Thus, **MORs** with a combination of functional-group based selectivity and a highly porous structure with defined pore size distribution, promise fast sorption kinetics and high efficiencies in practical separation processes. So far, there are limited reports on cationic metal–organic materials showing sorption capability for Cr(VI).[9] These examples show efficient Cr(VI) ion exchange capacity. However, all reported materials have been tested with batch methods and no studies on their use in columns have been carried out. Note that industrial wastewater processes require continuous bed flow ion exchange columns. A sorbent material, in order to be appropriate for use in such columns, should display (a) high selectivity and fast sorption kinetics for the targeted ion, (b) particle size suitable to allow continuous flow of wastewater through the column and (c) good mechanical strength to withstand high water pressures.[10] **MORs** and other porous materials are usually characterized by very small particle size and insufficient mechanical strength, which hinder their use in columns. Therefore, as-prepared **MORs** are not suitable for practical environmental remediation applications and thus, novel approaches are required in order to produce an engineered form of the materials to fulfil the requirements of column testing.

Herein we describe the anion exchange composite material based on the $[Zr_6O_4(OH)_4(NH_3^+\text{-BDC})_6]Cl_6$ **MOR** (**MOR-1**) and alginic acid (**HA**) polymer. The **MOR** is the analogue of the UiO-66 material containing NH_3^+ functional groups (Fig. 1).[11] Through detailed batch studies, the highly efficient and selective anion exchange properties of the composite for Cr(VI) are revealed. Importantly, for the first time, we demonstrate the successful use of **MORs**, in the form of **MOR–HA** composite, in an ion exchange column. The stationary phase in this column is a mixture of **MOR-1–HA** and sand (an inert and inexpensive material). Remarkably, a column with **MOR-1–HA**/sand stationary phase containing only 1% wt **MOR-1–HA** is capable to reduce moderate and trace levels of Cr(VI) well below the allowed safe levels defined by the USA-EPA (100 ppb)[3a] and EU (50 ppb),[3b] despite the presence of a large excess of competitive ions (Cl^-, Br^-, NO_3^-, SO_4^{2-} *etc.*). Furthermore, the column can be easily regenerated and reused several times with almost no loss of its capacity. The efficiency and simplicity of this ion exchange column make it attractive for use in the decontamination of wide variety of Cr(VI)-containing wastes.

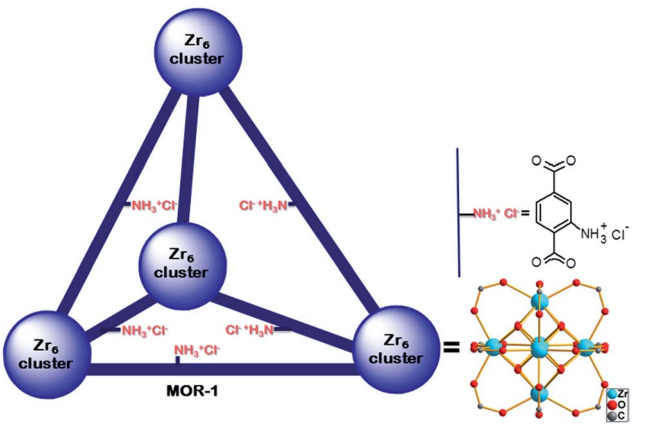

Fig. 1 Representation of the structure of (protonated) MOR-1 material shown as a tetrahedral cage (based on the structure of UiO-66 material[11]).

Results and discussion

Synthesis of MOR-1–HA composite

Zr^{4+} **MORs** of the UiO-66 family are very promising materials for sorption applications due to their high surface areas, easy incorporation of functional groups and hydrolytic-thermal stability.[11] However, as mentioned above, as prepared **MORs** as fine powders are not suitable for practical ion exchange applications. This is particularly true for UiO-66 type **MORs** usually isolated as nanoparticles (100–200 nm).[11g] The latter is a major drawback for the application of such materials as stationary phases in columns. To this end, we applied the alginate encapsulation method to prepare UiO-66 type-composite solids.[12] This encapsulation method (*method A*) involves (a) addition of the sorbent to be encapsulated (*i.e.* **MOR**) into an aqueous solution of sodium alginate (SA) so that one or more monolayers of alginate-saturated water cover each particle of the sorbent and (b) addition of $CaCl_2$ to the SA-sorbent suspension so that the monolayer is immediately converted to calcium alginate (CA), forming a water-insoluble polymer shell around the sorbent particulates (Fig. 2). Then, the **MOR-1–CA** material was treated with hydrochloric acid to produce $[Zr_6O_4(OH)_4(NH_3^+\text{-BDC})_6]Cl_6$–**HA** (**MOR-1–HA**) (**HA** = alginic acid) composite with protonated amine groups and extra-framework easily exchangeable Cl^- anions (see below), Fig. 2. Note that only 4% wt of alginate (*i.e.* alginate : **MOR-1** mass ratio used was ~0.04) is sufficient for the composite to be formed and thus, **MOR** is not encapsulated by thick **HA** particles that would hinder the diffusion of ions into the **MOR** pores. Alternatively, **MOR-1–HA** composite may be prepared directly by adding HCl into a suspension of **MOR-1** in SA aqueous solution (*method B*). The material synthesized with this method shows almost identical structural characteristics and ion-exchange properties with those of composite prepared with *method A*, as revealed by their very similar PXRD, IR and Cr(VI) ion-exchange isotherm data (see ESI†). However, for all studies described below, composite samples isolated with *method A* have been used.

Due to the presence of the **HA** shell covering the **MOR** particles, the composite **MOR-1–HA** material is not easily dispersed in water, in contrast to the pure **MOR-1** which forms a fine suspension upon mixing it with water (Fig. 3). This feature of the composite material is proved to be key for its successful utilization in ion-exchange columns (see below).

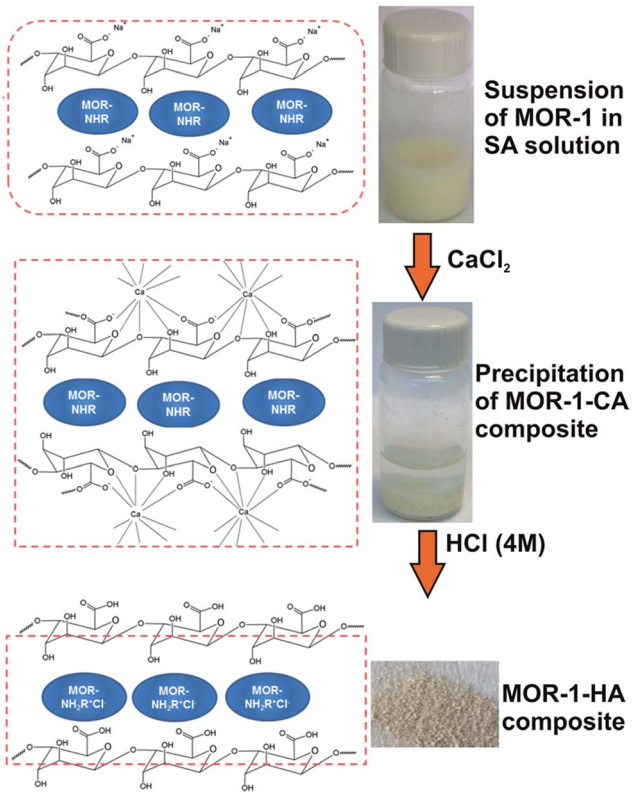

Fig. 2 Schematics for the preparation of the MOR-1–HA composite.

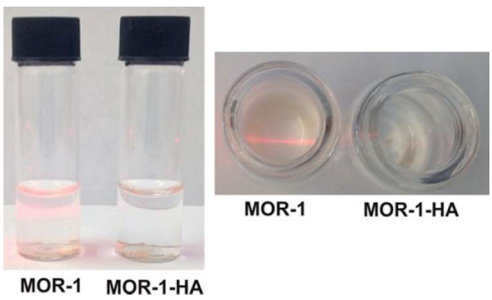

Fig. 3 Upon mixing MOR-1 with water a fine suspension is immediately formed (left vial), whereas MOR-1–HA is clearly separated from water (right vial). This is confirmed by the illumination of the mixtures with a laser pointer. Thus, the laser beam can be easily observed as it travels through the liquid in the left vial (Tyndall effect), whereas it is invisible when it travels through the clear solution in the right vial.

Characterization of MOR-1–HA composite

Scanning electron microscopy (SEM) images of **MOR-1–HA** and **MOR-1** particles indicate similar morphological characteristics for these materials (Fig. S1, ESI†). EDS analysis for the **MOR-1–HA** sample indicates a Zr : Cl ratio of ~1, which is in agreement with the protonation of the six amino-groups of the Zr_6 cluster and the presence of six Cl^- counter ions. Thermogravimetric analysis (TGA) was used for the determination of the lattice water molecules (21 H_2O molecules, Fig. S2†). Powder X-ray diffraction (PXRD) data indicate that the **MOR** retains its structure in the composite form (Fig. 4A).

The Brunauer–Emmett–Teller (BET) surface area of the **MOR-1–HA** was determined as 1004 $m^2\ g^{-1}$ (Fig. 4B), a value within the range of surface areas found for amino-functionalized UiO-66 materials.[11b,c] Analysis of CO_2 adsorption data with density function theory (DFT) gives a pore size of about 7 Å, (Fig. S3†).

Isolation and characterization of Cr(VI)-loaded material

Detailed Cr(VI) sorption studies for **MOR-1–HA** were performed at low pH (pH ~ 3), in order to model the usual acidic conditions of Cr(VI) industrial waste (for example tannery and metal plating wastewater).[13] Under such conditions, the predominant Cr(VI) species is $Cr_2O_7^{2-}$ (with some contribution from $HCrO_4^-$ at dilute solutions).[2b]

By immersing the **MOR-1–HA** material in a $Cr_2O_7^{2-}$ solution, the removal of $Cr_2O_7^{2-}$ is accomplished at a very fast rate (within a few minutes), an event that can be visually observed by the decolouration of the solution and colour change of the sorbent (Fig. S4†). This ion exchange process is described by the following equation:

$$[Zr_6O_4(OH)_4(NH_3^+\text{-BDC})_6]Cl_6\text{–HA} + 3Cr_2O_7^{2-} \rightarrow [Zr_6O_4(OH)_4(NH_3^+\text{-BDC})_6](Cr_2O_7)_3\text{–HA} + 6Cl^- \quad (1)$$

EDS data revealed no Cl^- anions in the Cr(VI)-loaded material **MOR-1–HA@Cr(VI)**. ICP-MS, EDS and UV-Vis data (see below) indicate a Zr : Cr ratio of 0.9–1.2, closed to the expected one (theoretical Zr : Cr = 1, considering the insertion of $3Cr_2O_7^{2-}$

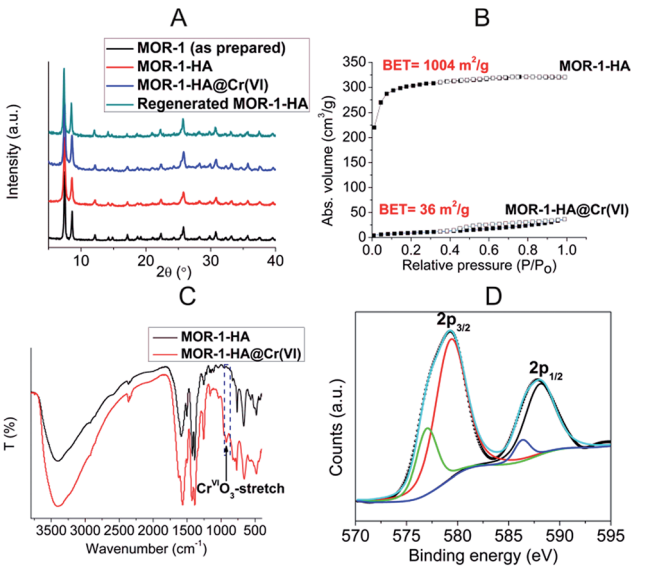

Fig. 4 (A) PXRD patterns of MOR-1 (as prepared), MOR-1–HA, MOR-1–HA@Cr(VI) and regenerated MOR-1–HA. (B) Nitrogen adsorption–desorption isotherms at 77 K for MOR-1–HA and MOR-1–HA@Cr(VI). (C) IR spectra of MOR-1–HA and MOR-1–HA@Cr(VI). (D) High-resolution Cr $2p_{1/2}$ and Cr $2p_{3/2}$ core-level photoelectron spectra of MOR-1–HA with their deconvolution into two components. The minor signals with binding energy at 586.3 and 577.0 eV are attributed to Cr(III) traces resulted from the known reduction effects under X-ray irradiation.[14]

per Zr_6 cluster). PXRD data revealed that the **MOR** structure is retained after the incorporation of the dichromate anions (Fig. 3A).

There is a drastic decrease, however, in the BET surface area for **MOR-1–HA@Cr(VI)** indicating the pores of the structure are filled by Cr(VI) species. Specifically, after the insertion of $Cr_2O_7^{2-}$ anions, the surface area for **MOR-1–HA** drops from ~1000 to 36 $m^2\ g^{-1}$ (Fig. 4B). Further evidence for the presence of Cr(VI) species in **MOR-1–HA@Cr(VI)** was provided by infrared (IR) and X-ray photoelectron spectroscopy (XPS). The IR spectrum (Fig. 4C and S5†) of the exchanged sample showed the existence of an absorption peak at ~924 cm^{-1} (not present in the spectra of pristine **MOR-1–HA** material) assigned to the antisymmetric $Cr^{VI}O_3$-stretch (for more detailed interpretation of IR data see also below). XPS data revealed the presence of Cr $2p_{1/2}$ and Cr $2p_{3/2}$ core-level signals, with their main components corresponding to binding energies of 588.1 and 579.3 eV (Fig. 4D). These binding energies are consistent with Cr(VI).[14]

Batch ion exchange studies

Ion-exchange equilibrium data. To gain further insight into the $Cr_2O_7^{2-}$ sorption properties of the **MOR-1–HA** material, we first performed batch ion exchange studies. The $Cr_2O_7^{2-}$ ion exchange equilibrium data for **MOR-1–HA** composite are shown graphically in Fig. 5. The description of the data can be provided by the Langmuir model (fitting also can be done with the Freundlich model, see ESI Fig. S6 and Table S1†).[15] The sorption capacity is 242 ± 17 mg $Cr_2O_7^{2-}$ per g of **MOR-1–HA** (or 242/0.96–252 mg g^{-1} of **MOR-1**, considering that **MOR-1–HA** contains 96% wt of **MOR-1**), which is well-comparable with the capacities of the best Cr(VI) sorbents.[7,9] This sorption capacity is consistent with the absorption of ~2.7 ± 0.2 moles of $Cr_2O_7^{2-}$ per formula unit of the **MOR-1**, which is close to the expected maximum sorption capacity of the material (3.0 mol per formula unit). The affinity of the **MOR-1–HA** for dichromate can be expressed in terms of the distribution coefficient K_d which is given by the equation

$$K_d = \frac{V\left[(C_0 - C_f)/C_f\right]}{m} \quad (2)$$

where C_0 and C_f are the initial and equilibrium concentration of $Cr_2O_7^{2-}$ (ppm), respectively, V is the volume (mL) of the testing solution and m is the amount of the ion exchanger (g) used in the experiment.[15] Values for K_d equal to or above 10^4 L g^{-1} are considered excellent. The maximum $K_d^{Cr_2O_7}$ values for the **MOR-1–HA**, obtained from the batch equilibrium studies, are in the range of (1.2–5.5) × 10^4 L g^{-1}, which reveal the exceptional affinity of this material for dichromate ions. We should also note that **MOR-1–HA** samples loaded with $Cr_2O_7^{2-}$ can be easily regenerated by treating them with concentrated HCl solutions (1.2–4 M). The PXRD pattern of the regenerated **MOF-1–HA** is almost identical with that of as prepared **MOR-1–HA** material (Fig. 4A). The regenerated **MOR-1–HA** showed similar dichromate exchange capacity (230–240 mg g^{-1}) as that of pristine material (more detailed regeneration studies were performed for the ion exchange columns, see below).

Kinetic studies. The kinetics of the $Cr_2O_7^{2-}$ exchange of the **MOR-1–HA** composite was also studied. The results indicate that the capture of $Cr_2O_7^{2-}$ by the composite was remarkably fast, as indicated by UV-Vis and ICP-MS data (Fig. 6). Within only 1 min of solution/composite contact, ~94.2% of the initial $Cr_2O_7^{2-}$ amount (C_0 = 21.6 ppm, pH ~ 3) was removed by the solution. After 3 min of solution/composite contact, the Cr(VI) ion exchange almost reached its equilibrium with ~97.5% removal capacity. These kinetic data can be fitted (Fig. 6B, inset) with the Lagergren's first-order equation

$$q_t = q_e[1 - \exp(-K_L t)], \quad (3)$$

where q_e = the amount (mg g^{-1}) of metal ion absorbed in equilibrium, K_L = the Lagergren or first-order rate constant (fitting parameters: q_e = 21.1 ± 0.4 mg g^{-1}, K_L = 3.3 ± 0.1 min^{-1}, R^2 = 0.90).[16] From these data, it is clear that the ordered highly porous structure of **MOR-1–HA** facilitating the diffusion of ions in and out of pores and the presence of protonated amine-functional groups strongly interacting with Cr(VI) (see theoretical studies below) result in a sorbent with exceptionally rapid sorption kinetics.

Variable pH studies. Although the Cr(VI) ion exchange studies for **MOR-1–HA** were mainly performed at pH ~ 3 in order to evaluate the capability of the sorbent to operate under acidic conditions usually present in industrial waste, the composite material is capable of absorbing Cr(VI) from solutions of a relatively wide pH range (1–8), Fig. 7. Specifically, it shows 91–98% total Cr removal capacities in pH ~ 3–8 (initial dichromate concentration = 21.6 ppm), whereas it retains high Cr removal capability even under highly acidic conditions (~81 and 90% removal capacities at pH ~ 1 and 2, respectively).

Selectivity studies. Cr(VI) bearing industrial effluent contains a number of competitive anions, such as Cl^-, NO_3^-, Br^- and SO_4^{2-}, in high concentrations. Thus, we have performed competitive $Cr_2O_7^{2-}/Cl^-$, $Cr_2O_7^{2-}/Br^-$, $Cr_2O_7^{2-}/NO_3^-$ and

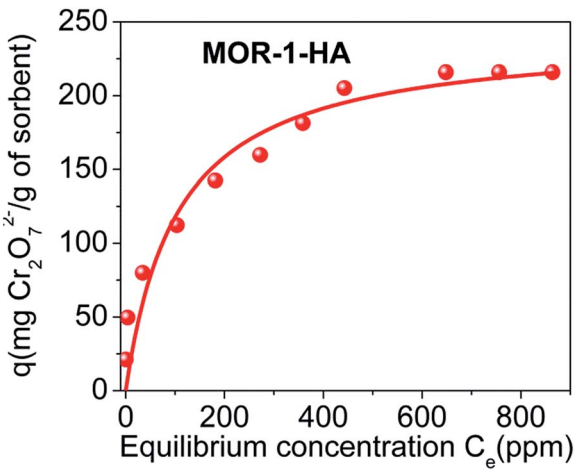

Fig. 5 Equilibrium $Cr_2O_7^{2-}$sorption data for MOR-1–HA material (pH ~ 3). The solid line represents the fitting of the data with the Langmuir model.

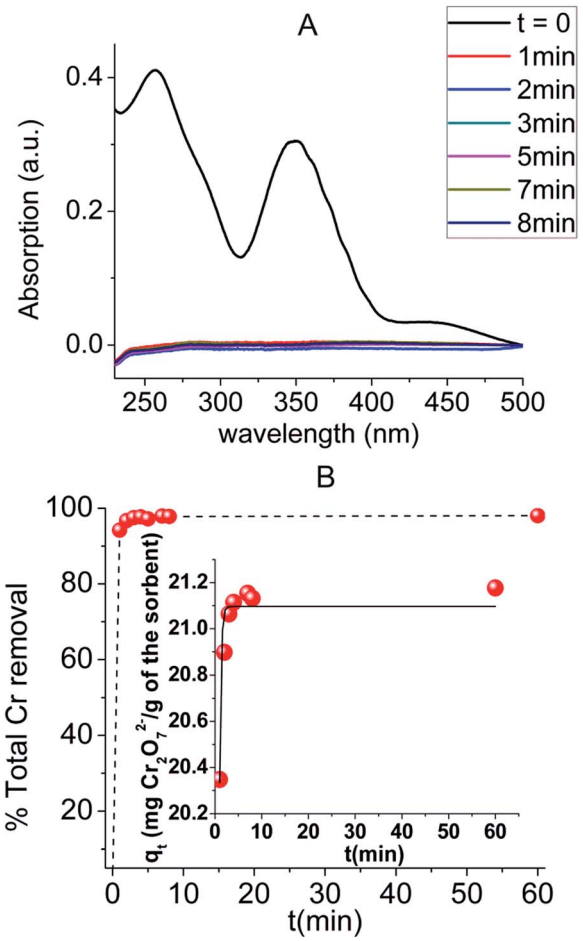

Fig. 6 (A) Selected UV-Vis data from the kinetic experiments (initial dichromate concentration = 21.6 ppm, pH ~ 3). The $Cr_2O_7^{2-}$ anions are not detectable after the sorption process with UV-Vis and thus, the dichromate concentrations of the solutions were determined by ICP-MS. (B) % Total Cr removal (determined by ICP-MS data) by **MOR-1–HA** *vs.* time (min). Inset graph: fitting of the kinetics data with the Lagergren's first-order equation.

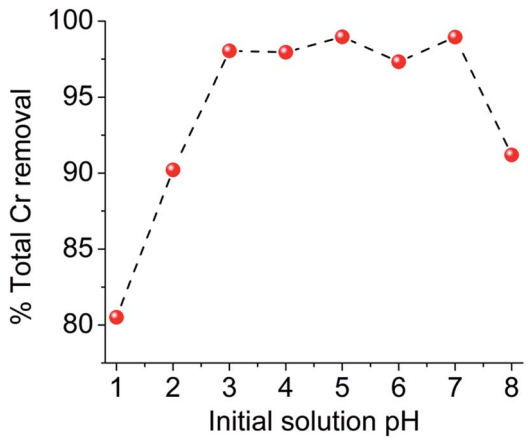

Fig. 7 % Total Cr removal (determined by ICP-MS data) by **MOR-1–HA** *vs.* pH (initial dichromate concentration = 21.6 ppm). For pH ≥ 9, dissolution of the composite was observed.

$Cr_2O_7^{2-}/SO_4^{2-}$ sorption experiments for **MOR-1–HA**. We have observed an exceptional ability of **MOR-1–HA** to absorb $Cr_2O_7^{2-}$ (initial concentration = 54 ppm, pH ~ 3) almost quantitatively (81.6–97.6% dichromate removal capacity) and very high $K_d^{Cr_2O_7}$ (4.4×10^3 to 4×10^4 L g^{-1}) in the presence of a tremendous (up to 1000-fold) excess of Cl^-, Br^-, or NO_3^-, which indicates the very high selectivity of **MOR-1–HA** for $Cr_2O_7^{2-}$ against these anions (Fig. S7 and Table S2†). SO_4^{2-} as a bivalent anion is expected to be stronger competitor than monovalent anions for dichromate anion exchange. Nevertheless, even with relatively large (20–80-fold) excess of SO_4^{2-}, **MOR-1–HA** retained a very good $Cr_2O_7^{2-}$ removal efficiency (40–68%) and relatively high $K_d^{Cr_2O_7}$ values (up to 2.1×10^3 mL g^{-1}) (Fig. S7 and Table S2†). By plotting $\log(K_d^{Cr_2O_7})$ *vs.* $\log(C_B)$ (C_B = concentration of Cl^-, Br^-, NO_3^- or SO_4^{2-} ions in mol L^{-1}), large selectivity coefficients[15] of **MOR-1–HA** for $Cr_2O_7^{2-}$ against Cl^-, Br^-, NO_3^- and SO_4^{2-} were observed (selectivity coefficient $K(Cr_2O_7^{2-}/Cl^-) = 200$, $K(Cr_2O_7^{2-}/Br^-) = 229$, $K(Cr_2O_7^{2-}/NO_3^-) = 224$, $K(Cr_2O_7^{2-}/SO_4^{2-}) = 159$, ESI†).

Comparative batch ion-exchange studies. For comparison, we have also performed batch $Cr_2O_7^{2-}$ sorption studies (at pH ~ 3) for (a) protonated **MOR-1** $[Zr_6O_4(OH)_4(NH_3^+\text{-BDC})_6]Cl_6$ (**MOR-1** treated with HCl 4 M), (b) non-protonated **MOR-1** $[Zr_6O_4(OH)_4(NH_2\text{-BDC})_6]$ (prepared without adding acid in the reaction mixture) and (c) **UiO-66 MOF** $([Zr_6O_4(OH)_4(BDC)_6])$–**HA** composite. The results indicate that the sorption capacities of protonated **MOR-1** and non-protonated **MOR-1** are similar to each other (247 ± 10 and 267 ± 23 mg g^{-1} respectively, Fig. S6 and Table S1†) and also close to that of **MOR-1–HA** composite, whereas the sorption capacity (129 ± 18 mg g^{-1}) of **UiO-66–HA** is almost half of that for **MOR-1–HA**. The efficiency, however, of protonated **MOR-1** and **MOR-1–HA** for sorption of dichromate in relatively low initial concentrations, as revealed by the $K_d^{Cr_2O_7}$ values, is significantly higher than that of non-protonated **MOR-1** and **UiO-66–HA**. Specifically, **UiO-66–HA** and non-protonated **MOR-1** materials show $K_d^{Cr_2O_7}$ values of 2.3 and 6.5×10^3 L g^{-1}, respectively, for initial dichromate concentration of ~21.6 ppm (Fig. 8), which are one order of magnitude less than those ($\sim 5.5 \times 10^4$ L g^{-1}) for **MOR-1–HA** and protonated **MOR-1** samples (Fig. 8).

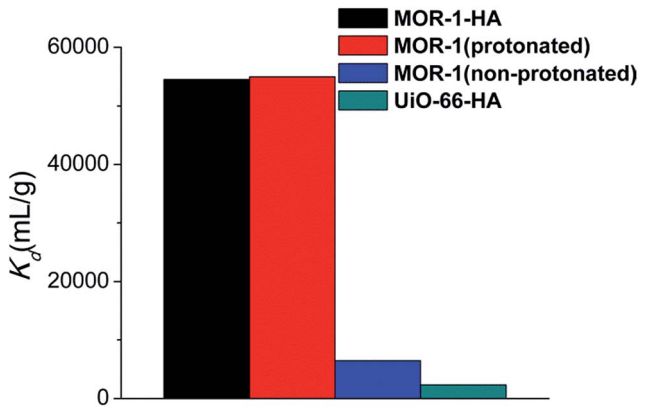

Fig. 8 K_d values for **MOR-1–HA**, **MOR-1** (protonated), **MOR-1** (non-protonated) and **UiO-66–HA** (initial dichromate concentration = 21.6 ppm).

As the above results revealed, both protonated and non-protonated **MOR-1** materials display similar maximum sorption capacities, since at the acidic environment the NH_2-groups will be eventually protonated and the inserted Cl^- can be exchanged by dichromate anions. However, at low initial Cr(VI) concentrations the materials pre-treated with acid (*i.e.* protonated **MOR-1** and **MOR-1–HA**) are much more effective for the sorption of Cr(VI) as revealed by their much higher K_d values compared to that of **MOR-1** used without any pre-treatment (non-protonated **MOR-1**). Presumably, the pre-existence of exchangeable Cl^- anions in the protonated materials enhances the kinetics of the Cr(VI) sorption, whereas the Cr(VI) sorption by the non-protonated **MOR** is a slower two-step process involving first protonation of the amine-sites/insertion of Cl^- anions and then exchange of Cl^- by Cr(VI) species. The enhancement of sorption kinetics is particularly important in the case of low initial Cr(VI) concentrations, which are not as effective as the high Cr(VI) levels at shifting the ion-exchange equilibrium towards the Cr(VI)-containing material. The above explanation is supported by the kinetic study of the $Cr_2O_7^{2-}$ exchange of the non-protonated **MOR-1** (Fig. S8†) using a relatively low initial dichromate concentration (21.6 ppm, pH $\sim$ 3). The results showed that after 1 min of solution/**MOR** contact only 24% $Cr_2O_7^{2-}$ removal is achieved, whereas even after 60 min of reaction significant amount of dichromate remains in the solution ($\sim$76% $Cr_2O_7^{2-}$ removal). These data are in contrast with the corresponding kinetic results for **MOR-1–HA** which indicated almost quantitative sorption of dichromate anions within only 1 min of solution/composite contact (Fig. 6). Furthermore, fitting of the kinetic data for the non-protonated **MOR-1** with the Lagergren's first order equation revealed a rate constant of 0.55 $\pm$ 0.14 min^{-1} (Fig. S8†), which is six-times smaller than that for the $Cr_2O_7^{2-}$ sorption by **MOR-1–HA**. This improvement of kinetics *via* the protonation of the material is the key for its substantially higher column sorption efficiency compared to that of non-protonated sorbent (see below).

Column ion exchange studies

The next step in our investigations was the study of the column Cr(VI) sorption properties of the **MOR-1–HA** material. At this point, we should mention that efforts to use as-prepared **MOR-1** (even after mixing it with inert materials such as sand) in columns, were unsuccessful since **MOR-1** forms fine suspensions in water that pass through the column (Fig. 9A). In contrast, **MOR-1–HA** composite is kept fixed in the column (Fig. 9B) and thus, it could be successfully employed for column sorption studies. The stationary phase in the columns was a mixture of **MOR-1–HA** and sand, a common inexpensive and inert material typically used in columns. The use of such mixtures instead of the pure composite has several advantages: (a) the pieces of the composite material are immobilized (not disturbed and moved by the water flow) and separated by particles of sand thus ensuring a continuous water flow through the column, (b) the pressure exerted by water on the composite will be reduced since part of this pressure will be absorbed by the second material (sand) and (c) mixing the composite material with a very low cost material such as sand is economically attractive. We should note that no clogging of **MOR-1–HA**/sand columns was observed after passing several liters of solutions through them. Remarkably, we found that stationary phases containing only $\sim$1% wt of **MOR-1–HA** and 99% wt sand are very effective for the removal of either high or low concentration Cr(VI) from aqueous solutions of various compositions. It can be seen that highly concentrated dichromate solution (C_0 = 1075 ppm, pH $\sim$ 3) is decolorized after passing it through the **MOR-1–HA**/sand column and also the stationary phase changed color from cream white to orange (red)-brown after the sorption of significant amount of $Cr_2O_7^{2-}$ anions (Fig. 10A and C). The sorbent can be easily regenerated by washing it with HCl solution (1.2–4 M) (Fig. 10B). The regeneration can be visually observed by the restoration of the cream white color of the initial **MOR-1–HA**/sand stationary phase (Fig. 10D).

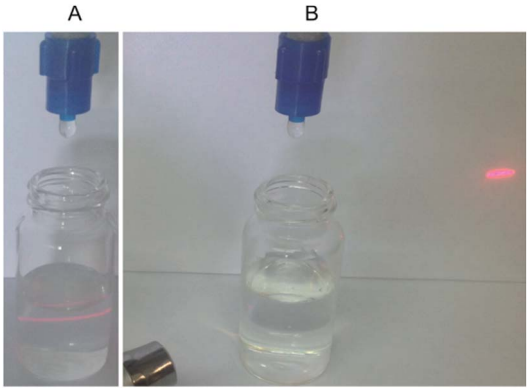

Fig. 9 (A) As-prepared **MOR-1**/sand column is washed with HCl acid (for protonation or regeneration of the sorbent) and then deionized water (to remove excess acid). As a result, **MOR-1** is coming through the column, since it forms a fine suspension as confirmed by the test with the laser beam. (B) The effluent collected after washing the **MOR-1–HA**/sand column with HCl acid and deionized water is a clear solution (as confirmed by the test with the laser beam).

Detailed column sorption studies were performed with $Cr_2O_7^{2-}$ solutions of relatively low or trace concentrations, which cannot be treated with common methods such as precipitation. Specifically, column sorption of a solution (pH $\sim$ 3) of dichromate anions with concentration of 6 ppm results in total Cr concentrations $\leq$ 47 ppb, which are below than the USA-EPA and EU allowed limits for total Cr in water, for 80 bed volumes (bed volume = [bed height (cm) $\times$ cross sectional area (cm^2)] mL) of the effluent (Fig. 11A). After regeneration, a breakthrough curve almost identical to that of the first run was obtained, whereas only a small decrease ($\sim$6 bed volumes) of the breakthrough capacity was observed after a fourth run of the column (Fig. 11A).

Column sorption studies have been also conducted with dichromate solutions (pH $\sim$ 3, C = 7 ppm) containing 100-fold excess of each of Cl^-, Br^- and NO_3^- anions. Still, the **MOR-1–HA**/sand column shows significant breakthrough capacity ($\sim$43 bed volumes) (Fig. S9†), a value which remains exactly the same after its regeneration.

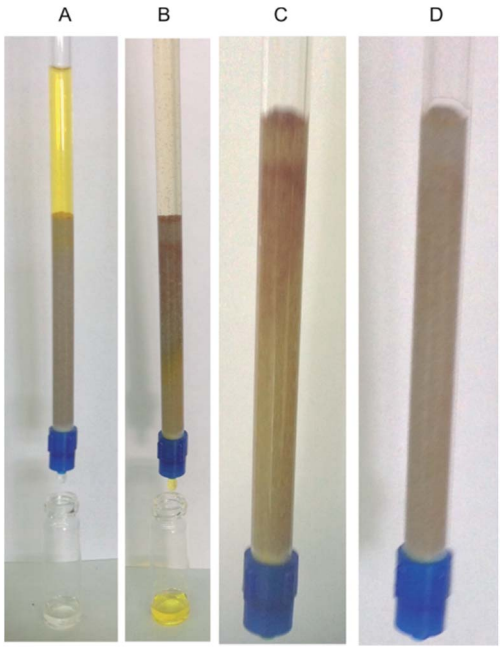

Fig. 10 (A) Decolouration of a $Cr_2O_7^{2-}$ solution (initial concentration = 1075 ppm, pH ~ 3) with an ion-exchange column of **MOR-1–A**/sand (0.05 : 5 g). (B) Regeneration of the $Cr_2O_7^{2-}$-loaded column by washing it with 4 M HCl solution. (C) Column with the stationary phase saturated with $Cr_2O_7^{2-}$. (D) Column after the regeneration process.

Because of the excellent $Cr_2O_7^{2-}$-column sorption properties described above, we decided to examine the applicability of **MOR-1–HA**/sand column for remediation of real-world water samples intentionally contaminated by trace concentrations of $Cr_2O_7^{2-}$. Specifically, we tested the performance of this ion exchange column for the decontamination of natural spring water solutions (with the pH of the solution adjusted to ~3) to which trace levels of $Cr_2O_7^{2-}$ (total Cr concentration analysed with ICP-MS ~450 ppb) were added. Note that the tested water solutions contain 27, 28 and 305-fold excess of SO_4^{2-}, NO_3^- and Cl^- anions, respectively, compared to the initial concentration of dichromate anions. The results indicated that at least 21 samples (bed volumes) collected after running the column three times (with regeneration of the column after each run) contain total Cr in a concentration ≤ 1 ppb, *i.e.* well below the allowed USA-EPA and EU levels for total Cr in water, Fig. 11B. We should also mention that no Zr was detected in the effluent samples (by ICP-MS analysis), thus excluding **MOR-1–HA** leaching from the column.

Finally, we investigated the performance of **MOR-1–CA**/sand column for dichromate sorption. The results revealed a breakthrough capacity of only 15 bed volumes (initial dichromate concentration = 6 ppm, pH ~ 3, **MOR-1–CA**/sand = 0.05 : 5 g, Fig. S10†) for this column, which is ~80% smaller than that of the **MOR-1–HA**/sand column (77 bed volumes, Fig. 11a). These data reflect the significantly enhanced Cr(VI) sorption kinetics for the protonated material (*i.e.* **MOR-1–HA**), as discussed above.

Mechanism of Cr(VI)-sorption

To provide an explanation for the remarkable selectivity of the protonated amino functionalized material for dichromate

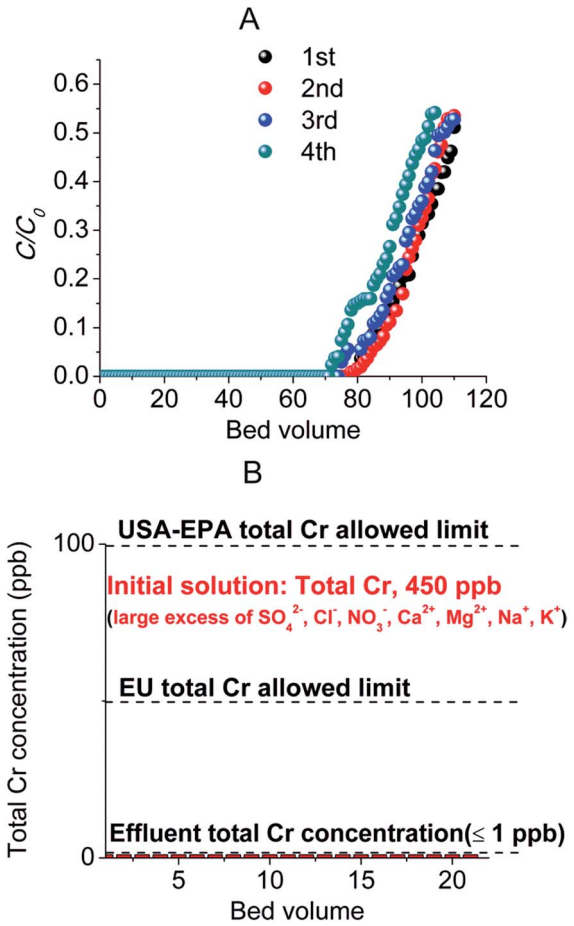

Fig. 11 (A) Breakthrough curves for four column ion exchange runs (C = concentration of the effluent, C_0 = initial $Cr_2O_7^{2-}$ concentration = 6 ppm, pH ~ 3, flow rate 1 mL min^{-1}, one bed volume = 3.5 mL, stationary phase **MOR-1–A**/sand = 0.05 : 5 g). (B) Total Cr concentration *vs.* bed volume (each bed volume = 3.5 mL) of natural spring water, to which trace Cr(VI) was added (initial total Cr concentration ~ 450 ppb, pH adjusted to 3), after passing the solution through an ion-exchange column of **MOR-1–A**/sand (0.05 : 5 g).

anions, we calculated the interaction energies of $Cr_2O_7^{2-}$, $HOCrO_3^-$, Cl^-, Br^-, NO_3^-, $HOSO_3^-$ and SO_4^{2-} anions with the $[Zr_6O_4(OH)_4(NH_3^+\text{-BDC})_6]Cl_6$–**HA** (**MOR-1–HA**), represented by the simple anilinium Ar-NH_3^+ cation, employing DFT methods (ESI†). The calculated interaction energies along with selected structural parameters of the respective associations are compiled in Table 1, while the optimized geometries and a brief description of them are given in the ESI (Fig. S11†).

Interestingly, our calculations indicate that SO_4^{2-} abstracts a NH_3^+ proton from the Ar-NH_3^+ cation yielding $HOSO_3^-$ anions *via* an exothermic process (exothermicity of −26.7 kcal mol^{-1}). Thus, in $Cr_2O_7^{2-}/SO_4^{2-}$ competition ion-exchange reactions with **MOR-1–HA**, the actual competitor for dichromate exchange was $HOSO_3^-$. The latter as a monovalent anion is expected to be less competitive than SO_4^{2-} for Cr(VI) sorption. This can be one of the reasons for the relatively high selectivity of **MOR-1–HA** for Cr(VI) *vs.* SO_4^{2-}, which was experimentally observed.

Table 1 Interaction energies, IE (in kcal mol^{-1}) and selected structural parameters (bond lengths R in Å, bond angles ∠ in degrees) for the Ar-NH_3^+···A (A = Cl^-, Br^-, NO_3^-, $HOSO_3^-$, $HOCrO_3^-$, $Cr_2O_7^{2-}$) associations in aqueous solutions calculated by the wB97XD/Def2-TZVPPD/PCM computational protocol

Anion	IE	R(O···H–N)	R(N–H)	∠O···H–N
Cl^-	11.7	1.942	1.070	176.1
Br^-	9.9	2.139	1.061	176.0
NO_3^-	13.3	1.597	1.071	175.7
$HOSO_3^-$	12.0	1.660	1.055	166.6
		2.478	1.020	110.3
$HOCrO_3^-$	12.6	1.672	1.052	159.4
		2.142	1.024	127.9
$Cr_2O_7^{2-}$	15.5	1.637	1.055	163.1

Among the anions studied, the $Cr_2O_7^{2-}$ anion shows the strongest interactions (15.6 kcal mol^{-1}). However, the estimated values of the interaction energies for the Ar-NH_3^+···A (A = Cl^-, Br^-, NO_3^-, $HOSO_3^-$, $HOCrO_3^-$, $Cr_2O_7^{2-}$) associations could not fully explain the high selectivity of the material under study towards $Cr_2O_7^{2-}$ anions and the limited selectivity for the rest of the competitive anions in the series. Therefore, this selectivity could be due to much stronger interactions between the $Cr_2O_7^{2-}$ anions and the Ar-NH_3^+ cation. Experimental IR-data indicate that the amine-deformation band is significantly red-shifted for **MOR-1–HA@Cr(VI)** (1565 cm^{-1}) compared to that for pristine **MOR-1–HA** (1590 cm^{-1}) and as prepared **MOR-1** (1580 cm^{-1}) samples (Fig. 4C and S5†).[17a,b] Furthermore, the IR peak at 1620 cm^{-1} (assigned to ring stretching vibration) in the spectrum of **MOR-1–HA@Cr(VI)**, which is also present in the IR spectrum of non-protonated **MOR** but it is not shown or is of very weak intensity in the spectrum of **MOR-1–HA**, is indicative of an NH_2- rather than NH_3^+-containing phenyl ring (Fig. S5†).[17c] In addition, the solid-state UV-Vis spectrum (Fig. S12†) for **MOR-1–HA@Cr(VI)** reveals a broad feature (around 500 nm) in the visible region (not shown in the spectrum of as-prepared **MOR-1** and **MOR-1–HA**) which may be due to charge transfer from the electron rich NH_2-BDC^{2-} ligand to Cr(VI) species (LMCT). The above support strong NH_2–Cr(VI) interactions in **MOR-1–HA@Cr(VI)**.

We thus suggest the transformation of dichromate to $Cr^{VI}O_3$ species which in turn forms the tetrahedral [(Ar-NH_2)CrO_3] complex.[18] To test this hypothesis, the equilibrium geometry of the [(Ar-NH_2)CrO_3] complex in aqueous solution was optimized at the wB97XD/Def2-TZVPPD level of theory, Fig. 12. The formation of such complex may be promoted by the significant acidity of anilinium ion (the pK_a of the anilinium ion is lower than 4.6). Anilinium may interact with the bridging O atom (nucleophilic center) of $Cr_2O_7^{2-}$ enforcing the rupture of a O–Cr bridging bond with concomitant coordination of aniline to the CrO_3 fragment and formation of $HOCrO_3^-$ anion. The latter subsequently re-equilibrates to produce $Cr_2O_7^{2-}$:

$$\text{Ar-NH}_3^+ + \text{Cr}_2\text{O}_7^{2-} \rightarrow \text{(Ar-NH}_2\text{)CrO}_3 + \text{HOCrO}_3^- \quad (4)$$

$$2\text{HOCrO}_3^- \rightarrow \text{Cr}_2\text{O}_7^{2-} + \text{H}_2\text{O} \quad (5)$$

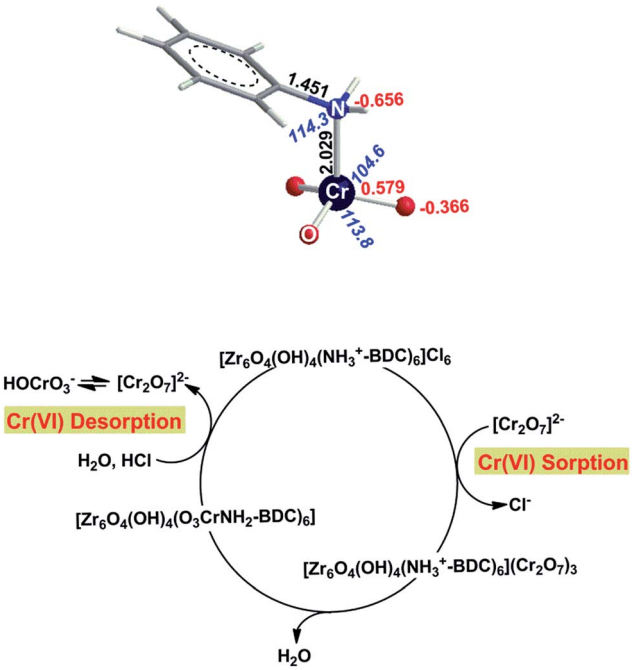

Fig. 12 Top: Equilibrium geometry of the (Ar-NH_2)CrO_3 complex in aqueous solution optimized at the wB97XD/Def2-TZVPPD level of theory along with selected structural parameters (bond lengths in Å and bond angles marked in blue in degrees) and the natural atomic charges (marked in red) on the donor atoms constituting the coordination sphere and the central Cr atom. Bottom: Suggested mechanism for the Cr(VI) sorption and desorption.

The condensation of the $HOCrO_3^-$ anion to form $Cr_2O_7^{2-}$ is particularly an enthalpy driven reaction with a dimerization constant $K = 159$ at standard conditions.[19]

The formation of the (Ar-NH_2)CrO_3 complex is an almost thermoneutral process, the endothermicity found to be 1.8 kcal mol^{-1}. The presence of six NH_3^+ functional groups per Zr_6 cluster affords six moles of the (Ar-NH_2)CrO_3 complex, thus accounting well for the experimentally observed sorption of ~3 moles of $Cr_2O_7^{2-}$ per formula unit of the **MOR** (Fig. 12).

Note that oxochromium(VI)-amine complexes are well-known compounds and many of them have been used as oxidants in organic synthesis.[20] The brick-red colour of the oxochromium(VI)-amine complexes[20] could account well for the change of colour from cream white to orange (red)-brown of the **MOR-1–HA** sorbent observed experimentally.

The regeneration of the **MOR-1–HA** columns by treating them with concentrated HCl solutions (1.2–4 M) can be easily explained by the acidic hydrolysis of the (Ar-NH_2)CrO_3 complex

$$\text{[(Ar-NH}_2\text{)CrO}_3\text{]} + \text{H}_2\text{O} \rightarrow \text{Ar-NH}_3^+ + \text{HOCrO}_3^- \quad (6)$$

with concomitant dimerization of $HOCrO_3^-$ to $Cr_2O_7^{2-}$ (Fig. 12). The exothermicity of the hydrolysis is predicted to be 30.5 kcal mol^{-1} at the wB97XD/Def2-TZVPPD level. The estimated binding energy of the aniline ligand with the CrO_3 moiety is 34.4 kcal mol^{-1}, while the negative natural atomic

charge on the coordinated N donor atom renders the N atom susceptible to electrophilic attack by the H^+ ions, which is transformed to ammonium NH_3^+ salt, thus regenerating the **MOR-1–HA** column.

Conclusions

Clearly, metal–organic resins (**MORs**) can be the next generation of resins, since their sorption capability is not only based on the functional-binding group (as occurs with the conventional organic resins) but also on their highly ordered porous structure enhancing the diffusion of ions and the sorption kinetics. Such materials, however, due to their very small particle size form fine suspensions in water, thus being not suitable for water treatment applications. We were able to overcome this limitation of **MORs** by engineering **MOR**–alginic acid (**HA**) composite form, in which the **MOR** particles are covered by a water-insoluble **HA** shell. Thus, the successful utilization of **MOR–HA** composite as stationary phase in ion-exchange columns was achieved. The excellent performance of such ion exchange columns, as demonstrated by their high efficiency for removal of Cr(VI) under a variety of conditions, points towards real-world environmental remediation applications of **MOR**-based sorbents.

Acknowledgements

The powder X-ray diffraction unit of the Network of Research Supporting Laboratories at the University of Ioannina is acknowledged. The work performed at Northwestern University was supported by National Science Foundation grant DMR-1410169.

References

1 E. A. Katayev, Y. A. Ustynyuk and J. L. Sessler, *Coord. Chem. Rev.*, 2006, **250**, 3004.
2 (*a*) M. Costa and C. B. Klein, *Crit. Rev. Toxicol.*, 2006, **36**, 155; (*b*) F. Brito, J. Ascanio, S. Mateo, C. Hernandez, L. Araujo, P. Gili, P. MartinZarza, S. Dominguez and A. Mederos, *Polyhedron*, 1997, **16**, 3846.
3 (*a*) USA-EPA. Chromium in drinking water, http://water.epa.gov/drink/info/chromium/; (*b*) European Commission. Council Directive 98/83/EC on the quality of water intended for human consumption, http://eur-lex.europa.eu/legal-content/EN/TXT/?uri=CELEX:31998L0083; (*c*) C. S. Peng, H. Meng, S. X. Song, S. Lu and A. Lopez-Valdivieso, *Sep. Sci. Technol.*, 2004, **39**, 1501.
4 (*a*) R. W. Liang, F. F. Jing, L. J. Shen, N. Qin and L. Wu, *J. Hazard. Mater.*, 2015, **287**, 364; (*b*) L. B. Hoch, E. J. Mack, B. W. Hydutsky, J. M. Hershman, I. M. Skluzacek and T. E. Mallouk, *Environ. Sci. Technol.*, 2008, **42**, 2600.
5 A. A. Zagorodni, *Ion Exchange Materials, Properties and Applications*, Elsevier, 2007.
6 M. J. McGuire, N. Blute, G. Qin, P. Kavounas, D. Froelich, and F. Leighton, *Hexavalent Chromium Removal Using Anion Exchange and Reduction with Coagulation and Filtration*, AWWA Research Foundation, 2007.
7 S. Kaneko and M. Ogawa, *Appl. Clay Sci.*, 2013, **75–76**, 109.
8 (*a*) M. Eddaoudi, D. B. Moler, H. L. Li, B. L. Chen, T. M. Reineke, M. O'Keeffe and O. M. Yaghi, *Acc. Chem. Res.*, 2001, **34**, 319; (*b*) G. Ferey, *Chem. Soc. Rev.*, 2008, **37**, 191; (*c*) S. Horike, S. Shimomura and S. Kitagawa, *Nat. Chem.*, 2009, **1**, 695; (*d*) D. Bradshaw, J. B. Claridge, E. J. Cussen, T. J. Prior and M. J. Rosseinsky, *Acc. Chem. Res.*, 2005, **38**, 273; (*e*) O. K. Farha and J. T. Hupp, *Acc. Chem. Res.*, 2010, **43**, 1166; (*f*) S. T. Zheng, T. Wu, J. A. Zhang, M. Chow, R. A. Nieto, P. Y. Feng and X. H. Bu, *Angew. Chem., Int. Ed.*, 2010, **49**, 5362.
9 (*a*) H. H. Fei, M. R. Bresler and S. R. J. Oliver, *J. Am. Chem. Soc.*, 2011, **133**, 11110; (*b*) H. H. Fei, C. S. Han, J. C. Robins and S. R. J. Oliver, *Chem. Mater.*, 2013, **25**, 647; (*c*) H. R. Fu, Z. X. Xu and J. Zhang, *Chem. Mater.*, 2015, **27**, 205; (*d*) X. X. Li, H. Y. Xu, F. Z. Kong and R. H. Wang, *Angew. Chem., Int. Ed.*, 2013, **52**, 13769; (*e*) P. F. Shi, B. Zhao, G. Xiong, Y. L. Hou and P. Cheng, *Chem. Commun.*, 2012, **48**, 8231; (*f*) Q. Zhang, J. Yu, J. Cai, L. Zhang, Y. Cui, Y. Yang, B. Chen and G. Qian, *Chem. Commun.*, 2015, **51**, 14732.
10 G. Tchobanoglous, F. L. Burton and H. D. Stensel, *Wastewater engineering: treatment, disposal, and reuse*, McGraw-Hill, 1991.
11 (*a*) J. H. Cavka, S. Jakobsen, U. Olsbye, N. Guillou, C. Lamberti, S. Bordiga and K. P. Lillerud, *J. Am. Chem. Soc.*, 2008, **130**, 13850; (*b*) M. J. Katz, Z. J. Brown, Y. J. Colon, P. W. Siu, K. A. Scheidt, R. Q. Snurr, J. T. Hupp and O. K. Farha, *Chem. Commun.*, 2013, **49**, 9449; (*c*) M. Kandiah, M. H. Nilsen, S. Usseglio, S. Jakobsen, U. Olsbye, M. Tilset, C. Larabi, E. A. Quadrelli, F. Bonino and K. P. Lillerud, *Chem. Mater.*, 2010, **22**, 6632; (*d*) A. J. Howarth, M. J. Katz, T. C. Wang, A. E. Platero-Prats, K. W. Chapman, J. T. Hupp and O. K. Farha, *J. Am. Chem. Soc.*, 2015, **137**, 7488; (*e*) K. K. Yee, N. Reimer, J. Liu, S. Y. Cheng, S. M. Yiu, J. Weber, N. Stock and Z. T. Xu, *J. Am. Chem. Soc.*, 2013, **135**, 7795; (*f*) C. B. He, K. D. Lu and W. B. Lin, *J. Am. Chem. Soc.*, 2014, **136**, 12253; (*g*) L. Zhu, D. Zhang, M. Xue, H. Li and S. Qiu, *CrystEngComm*, 2013, **15**, 9356; (*h*) W. Morris, W. E. Briley, E. Auyeung, M. D. Cabezas and C. A. Mirkin, *J. Am. Chem. Soc.*, 2014, **136**, 7261.
12 (*a*) A. I. Spjelkavik, Aarti, S. Divekar, T. Didriksen and R. Blom, *Chem.–Eur. J.*, 2014, **20**, 8973; (*b*) Y. H. Li, F. Q. Liu, B. Xia, Q. J. Du, P. Zhang, D. C. Wang, Z. H. Wang and Y. Z. Xia, *J. Hazard. Mater.*, 2010, **177**, 876; (*c*) M. G. Kanatzidis, D. Sarma and M. J. Manos, Column material for the capture of heavy metal and precious metal ions, *US Pat.*, 20150144568, 2015.
13 (*a*) M. Bosnic, J. Buljan, R. P. Daniels and S. Rajamani, *Pollutants in tannery effluent, published online*, 2003, http://leatherpanel.org/sites/default/files/publications-attachments/polutants.pdf; (*b*) F. Akbal and S. Camci, *Desalination*, 2011, **269**, 214.

14 (*a*) M. C. Biesinger, C. Brown, J. R. Mycroft, R. D. Davidson and N. S. McIntyre, *Surf. Interface Anal.*, 2004, **36**, 1550; (*b*) E. Desimoni, C. Malitesta, P. G. Zambonin and J. C. Riviere, *Surf. Interface Anal.*, 1988, **13**, 173.

15 (*a*) M. J. Manos, N. Ding and M. G. Kanatzidis, *Proc. Natl. Acad. Sci. U. S. A.*, 2008, **105**, 3696; (*b*) M. J. Manos and M. G. Kanatzidis, *J. Am. Chem. Soc.*, 2009, **131**, 6599; (*c*) M. J. Manos and M. G. Kanatzidis, *Chem.–Eur. J.*, 2009, **15**, 4779; (*d*) M. J. Manos and M. G. Kanatzidis, *J. Am. Chem. Soc.*, 2012, **134**, 16441; (*e*) M. J. Manos, V. G. Petkov and M. G. Kanatzidis, *Adv. Funct. Mater.*, 2009, **19**, 1087; (*f*) J. L. Mertz, Z. H. Fard, C. D. Malliakas, M. J. Manos and M. G. Kanatzidis, *Chem. Mater.*, 2013, **25**, 2116.

16 A. Benhammou, A. Yaacoubi, L. Nibou and B. Tanouti, *J. Colloid Interface Sci.*, 2005, **282**, 320.

17 (*a*) M. Karabacak, M. Cinar, Z. Unal and M. Kurt, *J. Mol. Struct.*, 2010, **982**, 22; (*b*) D. Lin-Vien, N. Colthup, W. Fateley and J. Grasseli, *The Handbook of Infrared and Raman Characteristic Frequencies of Organic Molecules*, Academic Press, 1991; (*c*) M. Tanaka and S. Ogasawar, *J. Catal.*, 1972, **25**, 111.

18 Two crystal structures of tetrahedral [$L(Cr^{VI}O_3$] complexes are reported in the following references: (*a*) M. R. Sundberg, R. A. M. Uggla, R. Sillanpaa, K. K. Zborowski, A. Sanchez-Gonzalez, J. K. T. Matikainen, S. A. A. Kaltia and T. A. Hase, *Cent. Eur. J. Chem.*, 2010, **8**, 486; (*b*) W. Mazurek, G. D. Fallon, P. J. Nichols and B. O. West, *Polyhedron*, 1990, **9**, 777.

19 F. Brito, J. Ascanio, S. Mateo, C. Hernandez, L. Araujo, P. Gili, P. MartinZarza, S. Dominguez and A. Mederos, *Polyhedron*, 1997, **16**, 3835.

20 (*a*) H. H. Sisler, J. D. Bush and O. E. Acoountius, *J. Am. Chem. Soc.*, 1948, **70**, 3827; (*b*) G. I. Poos, G. E. Arth, R. E. Beyler and L. H. Sarett, *J. Am. Chem. Soc.*, 1953, **75**, 422; (*c*) G. Tojo and M. Fernandez, *Oxidation of Alcohols to Aldehydes and Ketones*, Springer, Berlin, 2006, pp. 1–97.